Journal of Applied Fluid Mechanics, Vol. 1, No. 1, pp. 1-10, 2008.
Available online at www.jafmonline.net, ISSN 1735-3645.
DOI: 10.36884/jafm.1.01.11831

A Simple Solution of the Laminar Dam Break Wave

Hubert Chanson

Department of Civil Engineering, The University of Queensland, Brisbane QLD 4072, Australia

Email: h.chanson@uq.edu.au

(Received February 14, 2006; accepted August 7, 2006)

ABSTRACT

The sudden release of a mass of fluid in a channel generates a highly unsteady flow motion, called dam break wave. While industrial fluids exhibit sometimes non-Newtonian behaviours, the viscous fluid flow assumption remains a useful approximation for simplified analyses. In this study, new solutions of laminar dam break wave are proposed for a semi-infinite reservoir based upon the method of characteristics. The solutions yield simple explicit expressions of the wave front location, wave front celerity and instantaneous free-surface profiles that compare favourably with experimental observations. Both horizontal and sloping channel configurations are treated. The simplicity of the equations may allow future extension to more complicated fluid flows.

Keywords: Dam break wave, Laminar flow, Analytical solutions, Method of characteristics.

1. INTRODUCTION

A dam break wave is the result of a sudden release of fluid in a channel which may happen in various forms. The fluid may be clear-water, sediment-laden waters, muds and debris. Related situations include industrial applications with liquid concrete, some paints, some food liquid products, pasty sewage sludges and wastewater treatment residues (e.g. Coussot 1997, Tabuteau *et al.* 2004). In all applications, the surge front is a flow singularity characterised by a sudden discontinuity in flow depth and velocity. Hydraulic researchers conducted numerous studies of turbulent dam break wave experimentally (e.g. Schoklitsch 1917, Escande *et al.* 1961, Estrade and Martinot-Lagarde 1964) and analytically (e.g. Whitham 1955, Hunt 1982, 1984). A few studies considered laminar flow motion (e.g. Hunt 1994, Aguirre-Pe *et al.* 1995, Debiane 2000). Hunt (1994) developed an analytical solution for dam break wave down a sloping channel based upon a kinematics' wave approximation. Aguirre-Pe *et al.* (1995) studied both experimentally and numerically the flow on a sloping channel. Debiane (2000) considered both horizontal and sloping channel geometries. Piau (1996) analysed theoretically the dam break wave of an ideal fluid with yield stress, while Chanson *et al.* (2004) studied experimentally the dam break wave of thixotropic fluid down a sloping chute.

While some industrial fluids exhibit a non-Newtonian behaviour, the viscous fluid flow assumption (i.e. laminar regime) remains a useful approximation for simplified analyses. In this study, new analytical solutions are developed for laminar dam break waves. The results yield simple solutions for a semi-infinite reservoir with horizontal and sloping channels. The results are compared with some experimental data.

1.1 Fundamental Equations

For an unsteady open channel flow, the continuity and momentum equations yield a system of two

differential equations in terms of the depth-average velocity and flow depth. For a rectangular prismatic channel, the equations may be expressed in dimensionless terms as:

$$\frac{\partial d}{\partial t} + d\frac{\partial v}{\partial x} + v\frac{\partial d}{\partial x} = 0 \quad (1)$$

$$\frac{\partial v}{\partial t} + v\frac{\partial v}{\partial x} + \frac{\partial d}{\partial x} + \left(S_f - S_o\right) = 0 \quad (2)$$

where d is the dimensionless flow depth ($d = D/D_o$), D is the flow depth, D_o is the initial reservoir height (Fig. 1), t is the dimensionless time ($t = T\sqrt{g/D_o}$), T is the time, g is the gravity acceleration, x is the dimensionless distance from the dam wall ($x = X/D_o$), X is the streamwise co-ordinate, v is the dimensionless flow velocity ($v = V/\sqrt{gD_o}$), V is the depth-average velocity, S_o is the bed slope ($S_o = \sin\theta$), θ is the angle between the bed and the horizontal with $\theta > 0$ for a downward slope, and S_f is the friction slope (e.g. Liggett 1994, Montes 1998, Chanson 2004). The friction slope is the slope of the total energy line and it is defined as: $S_f = f/2 \times V^2/(gD_H)$ where D_H is the hydraulic diameter and f is the Darcy-Weisbach friction factor.

Equations (1) and (2) are called the Saint-Venant equations. They cannot be solved analytically usually because of non-linear terms (e.g. S_f). A mathematical technique to solve them is the method of characteristics. It yields a characteristic system of equations:

$$\frac{d}{dt}\left(v + 2c\right) = S_o - S_f \quad (3a)$$

$$\frac{d}{dt}\left(v - 2c\right) = S_o - S_f \quad (3b)$$

, along respectively:

$$\frac{dx}{dt} = v + c \quad \text{Forward characteristic C1 (4a)}$$

$$\frac{dx}{dt} = v - c \quad \text{Backward characteristic C2 (4b)}$$

where c is the dimensionless celerity of a small disturbance ($c = C/C_o$), C is the celerity of a small disturbance for an observer travelling with the flow ($C = \sqrt{gD}$ in rectangular channel) and $C_o = \sqrt{gD_o}$.

In the particular case of a frictionless dam break in a wide horizontal channel, equations (3) and (4) may be solved analytically (Ritter 1892). The dimensionless celerity of the dam break wave front equals:

$$u = 2 \quad (5)$$

, where $u = U/\sqrt{gD_o}$ and U is the wave front celerity. The dimensionless free-surface profile of an ideal dam break wave is a parabola:

$$\frac{x}{t} = 2 - 3\sqrt{d}, \qquad -1 \le \frac{x}{t} \le 2 \quad (6)$$

Ritter's solution is sketched in Fig. 1 (Top). Experimental observations showed however that laminar dam break waves propagate at a much slower pace than ideal fluid flow predictions. Further the leading edge of the wave has a rounded shape. These findings were confirmed by field observations of debris flow (e.g. Wan and Wang 1994, Wang 2002).

2. LAMINAR DAM BREAK WAVE IN A HORIZONTAL CHANNEL

The dam break flow is analysed as an ideal-fluid flow region behind a flow resistance-dominated tip zone (Fig. 1). Whitham (1955) introduced this approach for turbulent motion. Debiane (2000) used a similar model, but his development differs from the present simplified solution. The transition between the ideal dam break wave profile and the wave tip region is located at $x = x_1$ where the dimensionless water depth is $d = d_1$ (Fig. 1).

In the ideal fluid flow region, the basic equations yield the simple wave equations:

$$\frac{d}{dt}\left(v + 2c\right) = 0 \quad (7a)$$

$$\frac{d}{dt}\left(v - 2c\right) = 0 \quad (7b)$$

, along forward (Eq. (4a)) and backward (Eq. (4b)) characteristics.

In the wave tip region ($x_1 \le x \le x_s$), the flow velocity does not vary rapidly: experimental data showed that it is approximately the wave front celerity (Hunt 1994). Flow resistance is dominant, and the acceleration and inertial terms are small. The dynamic wave equation (Eq. (2)) may be reduced into a diffusive wave equation. For a horizontal channel, it yields:

$$\frac{\partial d}{\partial x} + \frac{f}{8}\frac{u^2}{d} = 0 \qquad \text{Wave tip region} \qquad (8)$$

, assuming a constant dimensionless velocity for $x_1 \leq x \leq x_s$. Basically, the slope of the free-surface becomes important to counterbalance the flow resistance next to the leading edge of the wave. Several researchers argued that the flow resistance in unsteady dam break wave flows may differ from classical steady flow estimates (e.g. Aguirre-Pe *et al.* 1995, Debiane 2000). It is assumed therefore that the flow resistance satisfies:

$$f = \alpha\frac{64}{\text{Re}} \qquad (9)$$

, where α is a correction factor and Re is the flow Reynolds number defined in terms of the hydraulic diameter D_H. For α=*1*, equation (9) yields the well-known steady flow result. For a wide channel (i.e. $D_H \approx 4D$), equation (9) may be rewritten in the wave tip region as:

$$f = \frac{16\alpha}{\mathbf{R}ud} \qquad (10)$$

, where

$$\mathbf{R} = \frac{\rho\sqrt{gD_o^3}}{\mu} \qquad (11)$$

is a reservoir flow Reynolds number that is a function of fluid properties and initial flow conditions only, and ρ and μ are the density and dynamic viscosity of the fluid respectively. The diffusive wave equation for the wave tip region (Eq. (8)) may be transformed. Its integration yields the shape of wave tip region for a laminar flow motion:

$$d = \sqrt[3]{6\alpha\frac{u}{\mathbf{R}}(x_s - x)}, \qquad x_1 \leq x \leq x_s \qquad (12)$$

, assuming a flow resistance correction coefficient α independent of the longitudinal distance *x*. Equation (12) is shown in Fig. 2 for two values of the correction coefficient α and compared with some experimental data.

At the transition between ideal fluid and friction-dominated wave tip region, the free-surface and velocity must be continuous. It yields two relationships:

$$d_1 = \frac{1}{9}\left(2 - \frac{x_1}{t}\right)^2 = \sqrt[3]{6\alpha\frac{u}{\mathbf{R}}(x_s - x)} \qquad (13a)$$

$$v_1 = u = \frac{2}{3}\left(1 + \frac{x_1}{t}\right) \qquad (13b)$$

, where the subscript *1* refers to the flow conditions at $x = x_1$ (Fig. 1).

The conservation of mass must be satisfied. The mass of fluid in the wave front region has to equal the mass of fluid in the ideal fluid flow profile for $x_1 \leq x$:

$$\int_{x_1}^{x_s} \sqrt[3]{6\alpha\frac{u}{\mathbf{R}}(x_s - x)}dx = \int_{x_1}^{2t} \frac{1}{9}\left(2 - \frac{x}{t}\right)^2 dx \qquad (14)$$

After substitution, the solution in terms of the dimensionless wave front celerity is:

$$\frac{1}{8\alpha}\mathbf{R}\frac{\left(1 - \frac{1}{2}u\right)^5}{u} = t \qquad (15)$$

The dimensionless wave front location is:

$$x_s = \left(\frac{3}{2}u - 1\right)t + \frac{1}{6\alpha}\frac{\mathbf{R}}{u}\left(1 - \frac{1}{2}u\right)^6 \qquad (16)$$

, and the entire free-surface profile equation satisfies:

$$\begin{aligned}
&d = 1, && x \leq -t \\
&d = \frac{1}{9}\left(2 - \frac{x}{t}\right)^2, && -t \leq x \leq \left(\frac{3}{2}u - 1\right)t \\
&d = \sqrt[3]{6\alpha\frac{u}{\mathbf{R}}\frac{x_s - x}{d_o}}, && \left(\frac{3}{2}u - 1\right)t \leq x \leq x_s \\
&d = 0, && x_s \leq x
\end{aligned} \qquad (17)$$

Equations (15) to (17) yield a complete analytical solution of the laminar dam break wave in a horizontal channel, while the location of the transition between wave tip and ideal flow is given by Eq. (13b). Typical longitudinal free-surface profiles are shown in Fig. 3 for several flow conditions. In Fig. 3b, Eq. (17) is plotted for three values of α and compared with experimental data. The graph shows that the correction term α has little influence on the front shape for $\alpha > 5$ to *10*.

3. EXTENSION OF THE SOLUTION TO A MILD-SLOPE CHANNEL WITH SOME INITIAL MOTION

The solution of the laminar dam break wave on a horizontal invert may be extended to a mild-slope channel including with some initial flow motion as

sketched in Fig. 4. Prior to dam break, the translation of both dam and reservoir is assumed frictionless. Dam break occurs at $t = 0$ when the dam wall is located at $x = 0$. After instantaneous wall removal, the flow is assumed to be an ideal fluid flow region behind a friction dominated wave tip region, while the translation of the undisturbed reservoir remains frictionless for $t > 0$.

In the ideal fluid flow region, equations (3) and (4) are applied assuming $S_f = 0$ (frictionless flow). Complete solutions for ideal dam break on sloping channel were presented by Peregrine and Williams (2001) and Chanson (2005). For a flat slope, the initial backward characteristic propagates upstream with a dimensionless celerity $(1\text{-}v_o)$ in first approximation, where v_o is the dimensionless initial reservoir translation velocity ($v_o = V_o/\sqrt{gD_o}$) and V_o is the initial reservoir translation speed (Fig. 4). Using the method of characteristics, the ideal fluid flow properties satisfy:

$$\begin{aligned} d &= \frac{1}{9}\left(2 + v_o + \frac{1}{2}S_o t - \frac{x}{t}\right)^2, \quad v_o - 1 \le \frac{x}{t} \le \frac{x_1}{t} \\ c &= \frac{1}{3}\left(2 + v_o + \frac{1}{2}S_o t - \frac{x}{t}\right), \quad v_o - 1 \le \frac{x}{t} \le \frac{x_1}{t} \\ v &= \frac{2}{3}\left(1 + \frac{1}{2}v_o + S_o t + \frac{x}{t}\right), \quad v_o - 1 \le \frac{x}{t} \le \frac{x_1}{t} \end{aligned} \tag{18}$$

, where S_o is positive for a downward slope.

In the wave tip region, the flow properties may be estimated using the diffusion wave equation taking into account flow resistance and bed slope:

$$\frac{\partial d}{\partial x} + \frac{f}{8}\frac{u^2}{d} - S_o = 0 \qquad \text{Wave tip region} \tag{19}$$

The solution of Eq. (19) gives the shape of the free-surface profile as:

$$x_s - x = \frac{1}{S_o}\left(\sqrt{2\frac{\alpha u}{S_o \mathbf{R}}}\,\tanh^{-1}\left(\frac{d}{\sqrt{2\frac{\alpha u}{S_o \mathbf{R}}}}\right) - d\right) \tag{20}$$

Equation (20) is shown in Fig. 5, where it is compared with experimental data and Eq. (12). On a mild slope, equations (20) and (12) yield almost identical results. Indeed, very close to the wave front, a Taylor series expansion of Eq. (20) yields Eq. (12) using the first two terms of the expansion only.

3.1 Simplified Solution

A simplified solution of the free-surface profile may be obtained assuming that the free-surface profile in the wave tip follows Eq. (12). The conservation of mass must be satisfied:

$$\begin{aligned} &\int_{x_1}^{x_s} \sqrt[3]{6\alpha \frac{u}{\mathbf{R}}(x_s - x)}\,dx = \\ &\int_{x_1}^{2(1+v_o/2+tS_o/4)t} \frac{1}{9}\left(2 + v_o + \frac{1}{2}S_o t - \frac{x}{t}\right)^2 dx \end{aligned} \tag{21}$$

The free-surface profile and velocity must be further continuous at the transition between the ideal fluid region and the friction dominated front region. After substitution, the exact solution of the dam break wave in terms of the dimensionless wave front celerity is:

$$\frac{\mathbf{R}}{8\alpha}\frac{\left(1 + \frac{1}{2}v_o + \frac{1}{2}S_o t - \frac{1}{2}u\right)^5}{u} = t \tag{22}$$

The dimensionless wave front location is:

$$\begin{aligned} x_s &= \left(\frac{3}{2}u - \frac{1}{2}v_o - S_o t - 1\right)t \\ &+ \frac{4}{fu^2}\left(1 + \frac{1}{2}v_o + \frac{1}{2}S_o t - \frac{1}{2}u\right)^4 \end{aligned} \tag{23}$$

, and the location of the transition between ideal and friction-dominated regions is given by:

$$x_1 = \left(\frac{3}{2}u - \frac{1}{2}v_o - S_o t - 1\right)t \tag{24}$$

Equation (22) provides an explicit relationship between the dimensionless wave front celerity and dimensionless time. The solution in terms of the wave front celerity is non-linear with the dimensionless time being present on both sides of Eq. (22). Equation (23) yields the dimensionless location of the wave front location as a function of the dimensionless wave front celerity and dimensionless time. Equations (18a), (12) and (24) gives the entire dimensionless free-surface profile $d = F(x/t)$.

4. DISCUSSION

4.1 Comparison with Experimental Data

The solutions were in qualitative agreement in terms of the wave front shape with the experimental data of Tinney and Bassett (1961), Aguirre *et al.* (1995) and Debiane (2000), and the analytical solution of

Hunt (1994). However further comparison is restricted by limited detailed flow measurements in viscous flow dam break waves, particularly on horizontal channels. Debiane (2000) presented a unique data set for laminar dam break wave in horizontal and sloping channels. He conducted basic experiments in a *3.0 m* long, *0.3 m* wide channel using glucose-syrup solutions of dynamic viscosities between *12* to *170 Pa.s*. During the early stages of the dam break, the dam break wave flow was similar to the flow conditions for an infinitely large reservoir and only this data set is considered herein for comparison: e.g., Figs. 2, 3 and 5.

Experiments with very viscous solutions may experience however some difficulties that were discussed by Debiane (Debiane 2000, pp. 161-163). Often the gate opening is relatively slow and cannot be considered to be an instantaneous dam break. Further, for very viscous solutions, some fluid is affected by the opening motion. Some fluid attaches to the gate while other portions are projected away. Debiane observed also sidewall effects for the most viscous solutions (μ = *170 Pa.s*) including some fluid crystallisation next to the walls at the wave front (Debiane 2000, p. 163). Overall the outcomes of these experimental problems are illustrated in Fig. 6 presenting a comparison between Debiane's data and analytical results in terms of dimensionless wave front locations for a laminar dam break motion in horizontal channel, an ideal dam break wave (Ritter's solution) and a turbulent dam break wave flow (Whitham 1955). The data showed systematically smaller dam break front celerity than theoretical predictions, including Ritter's solution (ideal fluid), Whitham's (1955) solution for turbulent flows, and theoretical solutions for laminar flows even with a flow resistance correction term α spreading over two orders of magnitude (Fig. 6).

4.2 Limitations of the Analytical Solutions

The present solutions are based upon a series of basic approximations. It is assumed that the wave tip region is primarily affected by bed friction while the ideal-fluid flow motion behind is mostly affected by inertial effects and the gravity force component. Further the development implies a mild bed slope because $c = 1$ is assumed on the initial backward characteristic, and the backward characteristics are assumed straight lines in the ideal fluid flow region.

A further approximation is some discontinuity of $\partial d/\partial x$ and $\partial V/\partial x$ at the transition between the wave tip region and the ideal fluid flow region, while the dimensionless bed shear stress f is discontinuous at both $x=x_1$ and $x=x_S$. Indeed the instantaneous distribution of the Darcy friction factor is:

$$\begin{aligned} f &= 16\alpha \frac{u}{\mathbf{R}} \frac{1}{d}, \quad x_1 \le x \le x_s \\ f &= 0, \qquad\qquad x < x_1 \end{aligned} \tag{24}$$

, and the dimensionless boundary shear stress becomes infinite at the wave front ($x = x_S$, $d = 0$).

5. CONCLUSIONS

New analytical solutions of the laminar dam break wave are proposed for a semi-infinite reservoir based upon the method of characteristics. The unsteady flow is analysed as a wave tip region where flow resistance is dominant, followed by an ideal-fluid flow region where inertial effects and gravity effects are predominant. The solutions yield simple explicit expressions of the wave front location, wave front celerity and instantaneous free-surface profiles. The results compare well with experimental observations, although these are limited and sometimes affected by experimental shortcomings.

The theoretical results yield explicit expressions that may be used to validate numerical solutions of the method of characteristics applied to the dam break wave problem. Dam break wave computations are indeed unstable next to the wave tip that is a flow singularity with zero water depth. Further the simplicity of the equations may allow some extension of the method to non-Newtonian fluid flows.

Finally it is acknowledged that the present approach is limited to semi-infinite reservoir, rectangular channel and quasi-instantaneous dam break.

REFERENCES

Aguirre-Pe, J., Plachco, F.P., and Quisca, S. (1995). "Tests and Numerical One-Dimensional Modelling of a High-Viscosity Fluid Dam-Break Wave." *Jl of Hyd. Res.*, IAHR, Vol. 33, No. 1, pp. 17-26.

Chanson, H. (2004). "The Hydraulics of Open Channel Flows : An Introduction." *Butterworth-Heinemann*, Oxford, UK, 2nd edition, 630 pages.

Chanson, H. (2005). "Applications of the Saint-Venant Equations and Method of Characteristics to the Dam Break Wave Problem." *Report No. CH55/05*, Dept. of Civil Engineering, The

University of Queensland, Brisbane, Australia, May, 135 pages.

Chanson, H. Jarny, S., Tocquer, L., and Coussot, P. (2004). "An Experimental Study of Sudden Release of Bentonite Suspensions down an Inclined Chute." *Proc. 15th Australasian Fluid Mech. Conf.*, AFMC, Sydney, Australia, M. Behnia, W. Lin & G.D. McBain Ed., Paper AFMC00252, 4 pages (CD-ROM).

Coussot, P. (1997). "Mudflow Rheology and Dynamics." *IAHR Monograph*, Balkema, The Netherlands.

Debiane, K. (2000). "Hydraulique des Ecoulements Laminaires à Surface Libre dans une Canal pour des Milieux Visqueux ou Viscoplastiques: Régimes Uniformes, Graduellement Varié, et Rupture de Barrage." *Ph.D. thesis*, University of Grenoble I, Rheology Laboratory INPG-UJF-CNRS, France, 273 pages.

Escande, L., NOUGARO, J., CASTEX, L., and BARTHET, H. (1961). "Influence de Quelques Paramètres sur une Onde de Crue Subite à l'Aval d'un Barrage." *Jl La Houille Blanche*, No. 5, pp. 565-575.

Estrade, J., and Martinot-Lagarde, A. (1964). "Ecoulement Consécutif à la Suppression d'un Barrage dans un Canal Horizontal de Section Rectangulaire." *Comptes-Rendus de l'Académie des Sciences de Paris*, Vol. 259, 21 December, Group 2, pp. 4502-4505.

Hunt, B. (1982). "Asymptotic Solution for Dam-Break Problems." *Jl of Hyd. Div.*, Proceedings, ASCE, Vol. 108, No. HY1, pp. 115-126.

Hunt, B. (1984). "Perturbation Solution for Dam Break Floods." *Jl of Hyd. Engrg.*, ASCE, Vol. 110, No. 8, pp. 1058-1071.

Hunt, B. (1994). "Newtonian Fluid Mechanics Treatment of Debris Flows and Avalanches." *Jl of Hyd. Engrg.*, ASCE, Vol. 120, No. 12, pp. 1350-1363.

Liggett, J.A. (1994). "Fluid Mechanics." *McGraw-Hill*, New York, USA.

Peregrine, D.H., and Williams, S.M. (2001). "Swash Overtopping a Truncated Plane Beach." *Jl of Fluid Mech.*, Vol. 440, pp. 391-399.

Piau, J.M. (1996). "Flow of a Yield Stress Fluid in a Long Domain. Application to Flow on an Inclined Plane." *Jl of Rheology*, Vol. 40, No. 4, pp. 711-723.

Ritter, A. (1892). "Die Fortpflanzung der Wasserwellen." *Vereine Deutscher Ingenieure Zeitschrift*, Vol. 36, No. 2, 33, 13 Aug., pp. 947-954.

Schoklitsch, A. (1917). Über Dambruchwellen." *Sitzungberichten der Königliche Akademie der Wissenschaften, Vienna*, Vol. 126, Part IIa, pp. 1489-1514.

Tabuteau, H., Baudez, J.C., Bertrand, F., and Coussot, P. (2004). "Mechanical Characteristics and Origin of Wall Slip in Pasty Biosolids." *Rheol. Acta*, Vol. 43, pp. 168-174.

Tinney, E.R., and Bassett, D.L. (1961). "Terminal Shape of a Shallow Liquid Front." *Jl of Hyd. Div.*, Proceedings, ASCE, Vol. 87, No. HY5, pp. 117-133.

Wan, Zhaohui, and Wang, Zhaoyin (1994). "Hyperconcentrated Flow." *Balkema*, IAHR Monograph, Rotterdam, The Netherlands, 290 pages.

Wang, Z.Y. (2002). "Initiation and Mechanism of Two Phase Debris Flow." *Proc. Conf. on Flood Defence'2002*, Ed. WU *et al.*, Science Press, New York, pp. 1637-1648.

Whitham, G.B. (1955). "The Effects of Hydraulic Resistance in the Dam-Break Problem." *Proc. Roy. Soc. of London*, Ser. A, Vol. 227, pp. 399-407.

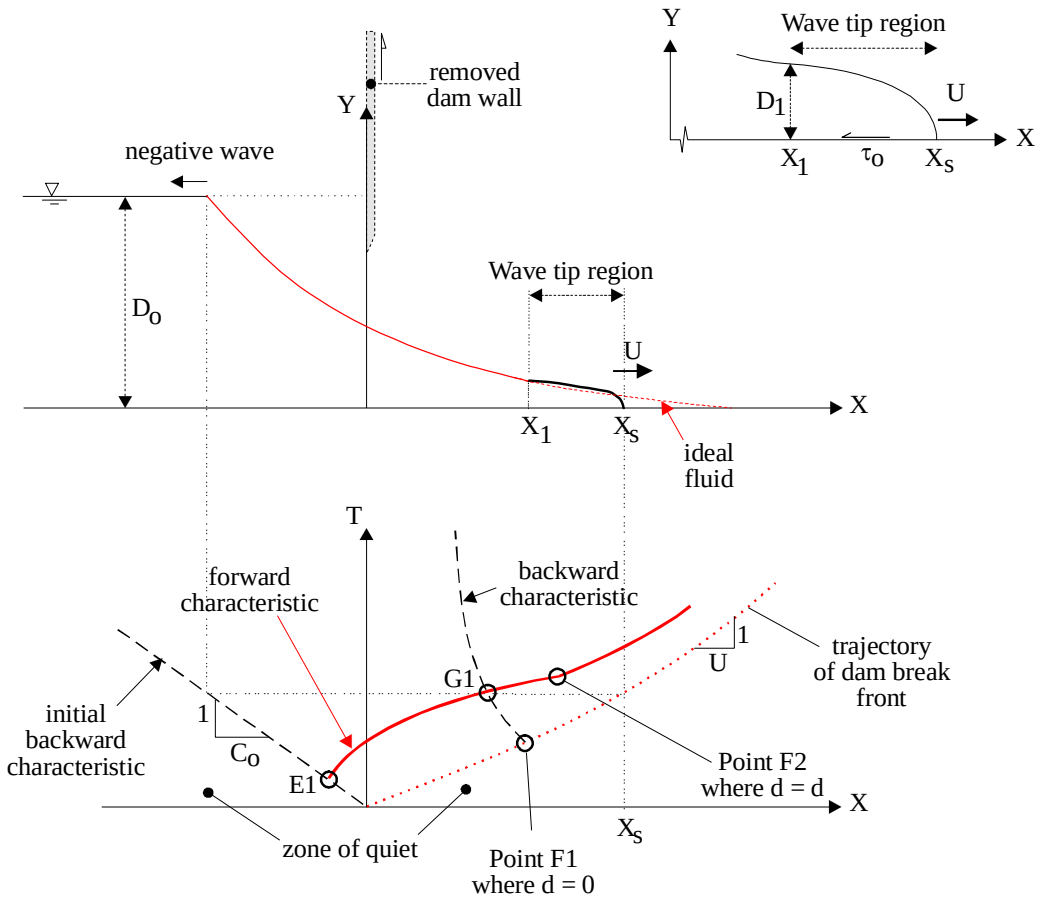

Fig. 1 - Sketch of dam break wave in a horizontal dry channel.

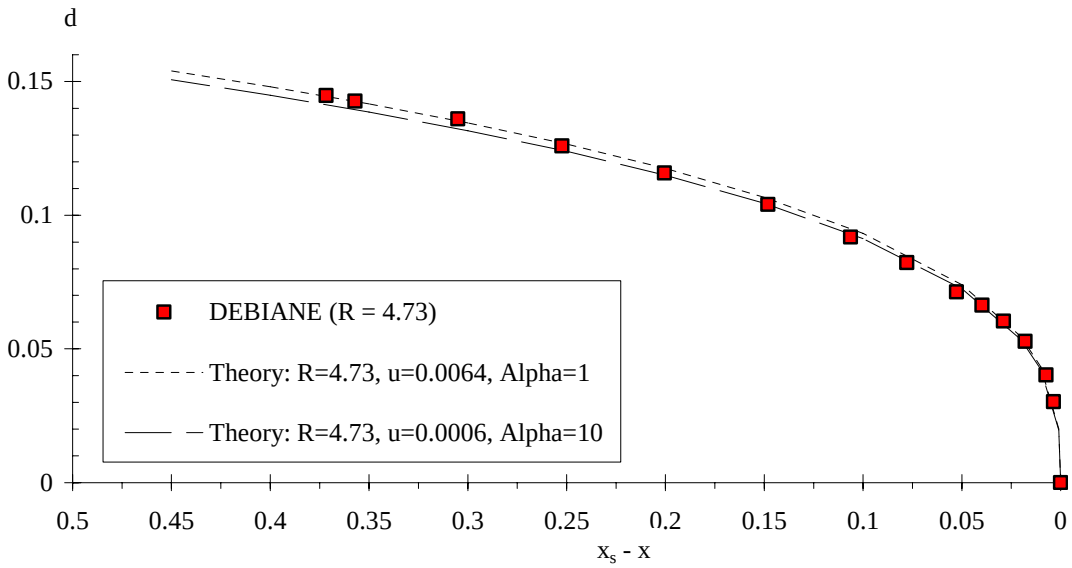

Fig. 2 - Wave front shape for a dam break wave in a dry horizontal channel - Comparison between Eq. (12) and experimental data (Debiane 2000, **R** = *4.73, t = 5620, S_o = 0*).

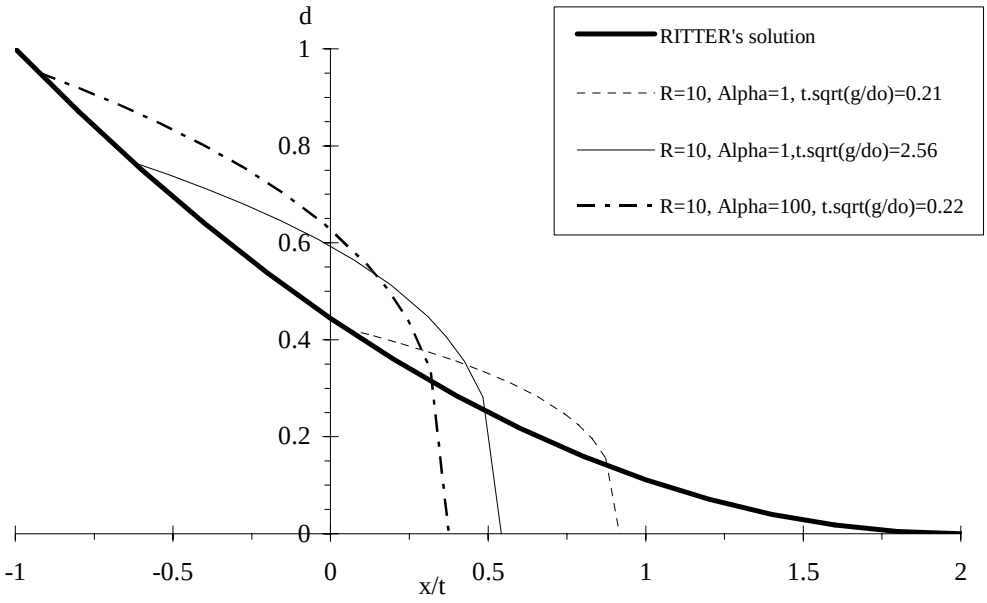

(a) Instantaneous dimensionless free-surface profile (Eq. (17)) for **R** = *10* and α = *1* and *100.*

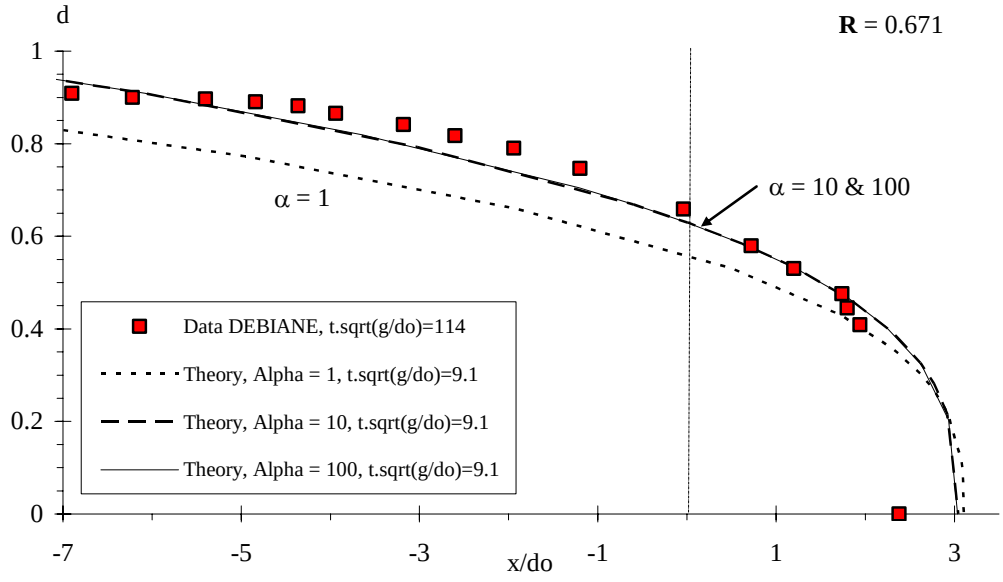

(b) Instantaneous free-surface profile for **R** = *0.671* - Comparison between Debiane's data (*t* = *114*) and Eq. (17) (for *t* = *9.1*, α = *1*, *10* and *100*).

Fig. 3 - Dimensionless free-surface profile solutions for laminar dam break wave (horizontal channel, zero initial motion).

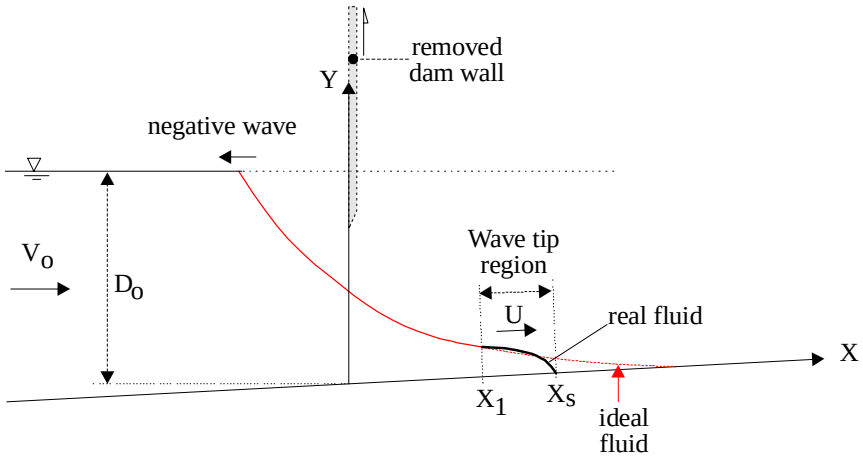

Fig. 4 - Sketch of dam break wave in a sloping channel with initial flow motion.

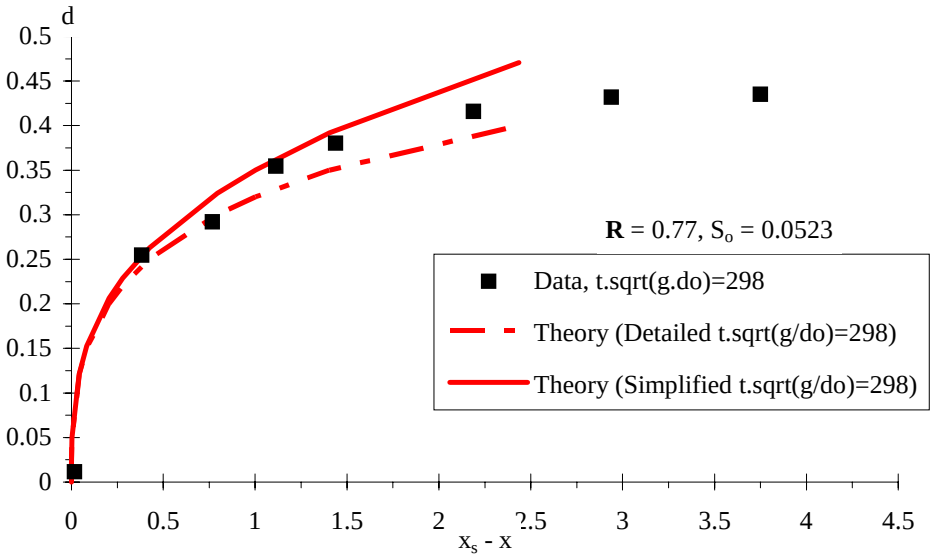

Fig. 5 - Wave front shape for a dam break wave in a sloping channel - Comparison between Eq. (20) (Detailed solution), Eq. (12) (Simplified solution) and experimental data (Debiane 2000, **R** = *0.77, t = 298,* S_o *= 0.0523*).

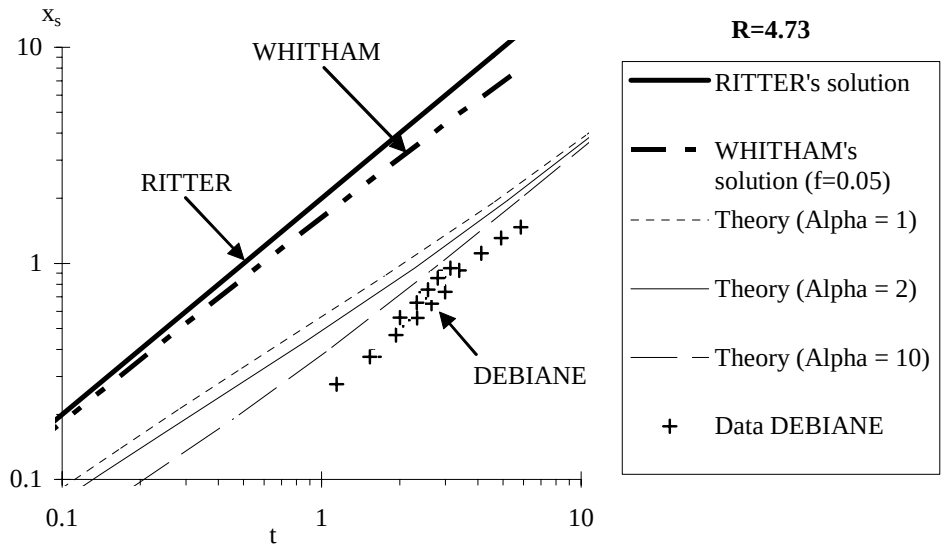

Fig. 6 - Wave front location for a dam break wave in a horizontal channel - Comparison between ideal fluid flow calculations (Ritter's solution), turbulent flow calculations (Whitham 1955), laminar flow calculations (Eq. (16)) and experimental data (Debiane 2000, **R** = *4.73*, S_o = *0*)